Estimation of thermal effects on receptor from pool fires

Zuzana Labovská, Juraj Labovský

Institute of Chemical and Environmental Engineering, Faculty of Chemical and Food Technology, Slovak University of Technology in Bratislava
zuzana.labovska@stuba.sk

Abstract: The aim of this contribution is to provide an overview of the calculation procedures of risk analysis, that is, the effects and consequences of pool fires. Fires and explosions are the most significant and most common causes of damage to equipment and of injuries and death in industry. Damages are a direct consequence of the generated heat flux. Mathematical tools for the prediction of heat flux at a distance can be divided into four classes: semi-empirical models, field models, integral models and zone models. Semi-empirical modeling is a relatively simple technique providing models predicting heat flux at a distance. There are two types of semi-empirical models: point source models and surface emitter models. By their nature, semi-empirical models depend strongly on experimental data. Correlations are able to describe the general features of a fire. Semi-empirical models are ideal for routine hazard assessment purposes because they are mathematically simple, and hence easily understood. However, if more models describing the same phenomenon are available, significant differences in the heat flux prediction can be expected. In this contribution, differences in the prediction of the heat flux from pool fires are discussed.

Keywords: flame dimensions, pool fire, release of flammable chemicals, risk analysis, thermal effect on receptor

Introduction

Fire is an exothermic oxidation reaction occurring in the gas phase which results from the mixing of flammable gases with air or other oxidative agents. When the concentration of the flammable substance reaches its critical mass for ignition and a proper ignition source capable of supplying the required power is present, a fire will start. Fire (pool fire on land or on water, jet fire, flash fire, fireballs) is the most significant and most common cause of damage to equipment and injuries and death in chemical industry. Damages are a direct consequence of the generated heat flux and the toxic gases produced by combustion. Heat flux, E_r, from the flame surface can be easily described by the Stefan-Boltzmann equation:

$$E_r = \varepsilon\sigma\left(T_f^4 - T_a^4\right) \quad (1)$$

where ε denotes the grey-body emissivity, σ the Stefan-Boltzmann constant ($\sigma = 5.6704 \times 10^{-8}\,\mathrm{W\,m^{-2}\,K^{-4}}$), and temperatures T_f and T_a refer to the temperature at the flame surface and the ambient temperature, respectively. However, since the temperature differs throughout the flame and hence an overall flame surface temperature cannot be determined, equation (1) cannot be used to reliably predict the heat flux from the flame surface. Moreover, the flame does not radiate heat from its whole surface since a part of it is covered by soot and a large part of the heat flux is absorbed by carbon dioxide and water present in the atmosphere. For these reasons, the heat flux calculated by the Stefan-Boltzmann equation is significantly higher than the real heat flux on the receptor (Assael, 2010). The main aim of thermal effect modeling is to estimate possible injury or damage to people and objects from thermal radiation from an incident outcome (GCPQRA, 2000). The probit models estimate fatality levels for a given thermal dose from fires. Fatal thermal dose depends on the exposure duration and on the intensity of heat flux. The higher the heat fluxes on the receptor, the shorter the exposure necessary to reach the same level of fatalities (Fig. 1). It is clear that heat flux at receptor is significantly dependent on the distance between the receptor and the flame. So, the crucial moment of the estimation of the thermal effect on receptor is the determination of the heat flux at a defined distance or of the distance in which the heat flux is dangerous for the receptor.

Theoretical

Mathematical models

In an effort to estimate the heat flux and its effects, many models have been introduced in literature. Mathematical tools for the prediction of the heat flux at a distance can be divided into four classes:

– Semi-empirical models – relatively simple models for the prediction of heat flux at a distance. Most semi-empirical models of flames focuse on the prediction of flame shapes (location of a fire in

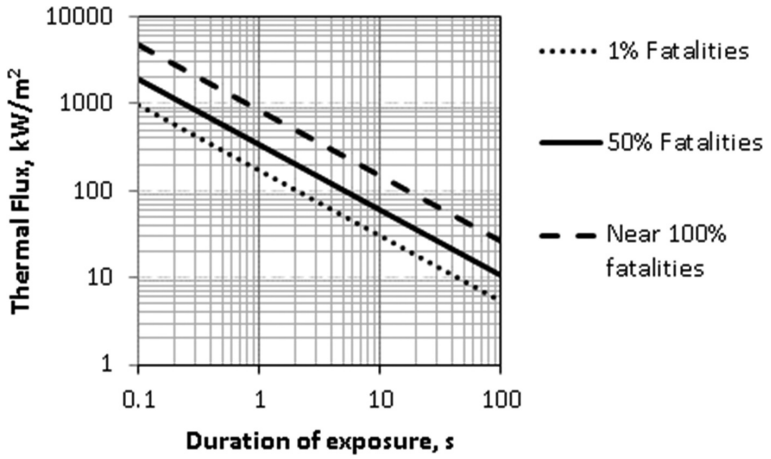

Fig. 1. Fatality levels for different exposure duration and heat flux at receptor, calculated using the Eisenberg et al. (1975) probit model.

space, flame length and tilt) and heat fluxes to external objects and they strongly depend on experimental data (CRP 14E, 1997).

- Field models — or computational fluid dynamics models (CFDs), are based on the numerical solution of the partial differential Navier-Stokes equations. The main disadvantage of these models is in the immense requirements on computing time, difficult programming and incompatibility with many applications (Assael, 2010).
- Integral models — a compromise between the semi-empirical models and the CFD models; they incorporate a more rigorous description of the physics than semi-empirical models because they are formulated mathematically in the same way as field models and are based on the solution of differential equations for the conservation of mass, momentum and energy. In this way, a significant reduction in the computing time is achieved (CRP 14E, 1997).
- Zone models — are employed in structural areas but not in open spaces. According to the zone models, space is separated into homogeneous space zones of unified approach connected by empirical equations and mass and energy balances (Assael, 2010).

Considering the aforementioned methods, semi-empirical models are the most widely used for routine hazard estimation because they are easily understood and mathematically uncomplicated. There are two types of semi-empirical models:

- Point source models, which do not consider the shape of the flame because heat-flux is assumed to originate from a point source located in the center of flame.
- Solid plume radiation models, which assume that heat is radiated from the surface of a flame described as a solid object (cylinder or cone).

Semi-empirical models for pool fire heat flux calculation

Pool fire semi-empirical models are composed of several submodels as it is very schematically shown in Fig. 2. Calculation of some parameters (burning rate, maximum pool diameter, flame length) does not depend on the type of the semi-empirical model and the values of these parameters can be used in the point source model as well as in the solid plume radiation model.

Burning Rate

Burning rate expresses the rate with which the flammable material that forms the pool burns and can be calculated applying several methods, e.g.:

- Zabetakis-Burgess method (Zabetakis and Burgess, 1961),
- Burgess-Strasser-Grumer method (Burgess et al. 1961),
- Mudan method (Mudan, 1985).

The Zabetakis-Burgess method determines the pool burning rate as:

$$m_B = m_{B\infty}\left(1 - e^{-k\beta D}\right) \tag{2}$$

in which $m_{B\infty}$ is the burning rate of an infinite diameter pool, D is pool diameter, k is absorption extinction coefficient of the flame, β refers to the mean beam length corrector and $(1 - e^{-k\beta D})$ represents the effective flame volume emissivity. The difference between m_B and $m_{B\infty}$ decreases below 10 % if the pool diameter is above 2 meters (CRP 14E, 1997).

According to the Burgess-Strasser-Grumer method, the burning rate, m_B, can be calculated from the expression:

$$m_B = \dot{y}_{\max}\rho_{liq} \tag{3}$$

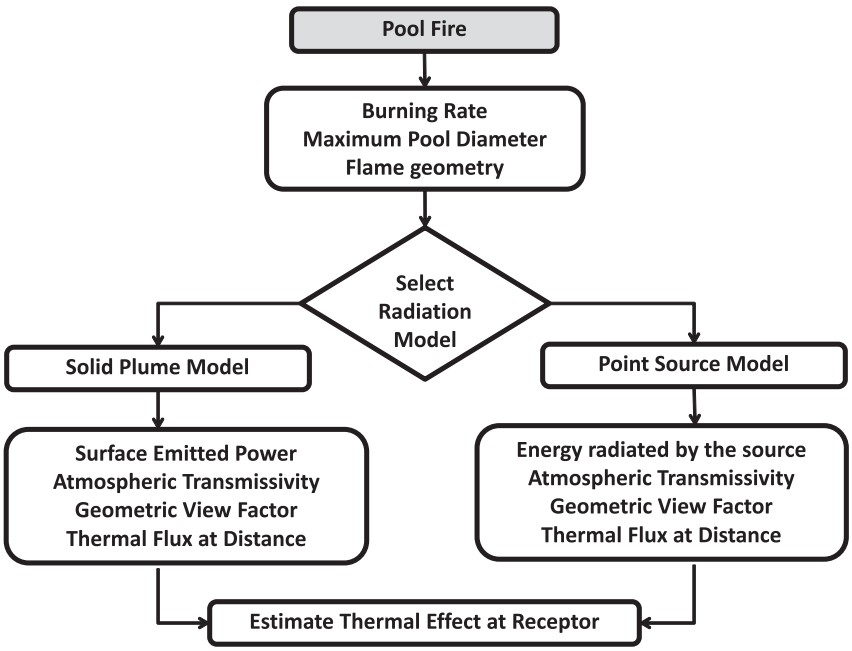

Fig. 2. Logic diagram for pool fire radiation effects calculation.

where ρ_{liq} is the fuel density and $\dot{y}_{\max}$ is the vertical rate of the liquid level decrease:

$$\dot{y}_{\max} = 1{,}27.10^{-6} \frac{\Delta H_c}{\Delta H_v + \int_{T_a}^{T_{BP}} C_p dT} \tag{4}$$

where T_{BP} is fuel boiling point temperature and ΔH_c and ΔH_v refer to the heat of combustion and the heat of vaporization, respectively. This method provides good results for the calculation of the burning rate of hydrocarbons and liquid fuels in general, but it underestimates the burning rate of liquefied gases (Assael, 2010).

Maximum pool diameter

For a continuous leak on an infinite flat plane, the maximum diameter, $D_{\max}$, is reached when the product of the burning rate and the surface area equals the leakage rate, $\dot{V}_L$:

$$D_{\max} = 2\sqrt{\frac{\dot{V}_L}{\pi \dot{y}_{\max}}} \tag{5}$$

In case of an instantaneous leak of defined volume of flammable material, V_L, the pool diameter, D, depends on the pool thickness, δ:

$$D = 2\sqrt{\frac{V_L}{\pi \delta}} \tag{6}$$

In most cases, pool size is fixed by the local physical barriers (e.g. dikes, sloped drainage areas). Circular pools are normally assumed; when dikes lead to square or rectangular pool shapes, an equivalent diameter can be used.

Flame geometry

The most important parameters of a burning pool which determine the flame shape are the flame length, flame tilt and less often the flame drag. Many observations of pool fires show that there is an approximate ratio of the flame height to diameter (*L/D*). For example, Lees (1994) suggested a value of the *L/D* ratio of 2. The best known correlation of this ratio has been given by Thomas (1963) for still air conditions and by Moorhouse (1982), which includes the effect of wind on the flame length. Table 1 provides an overview of the pool fire flame length correlations, where correlation, ρ_a, represents the density of air at ambient conditions and g the acceleration due to gravity. The nondimensional wind speed, u^*, is directly related to the wind velocity, u_W, at a 10 m height, as:

$$u^* = \frac{u_W}{\left[\left(g m_B D\right) / \rho_a\right]^{1/3}} \tag{7}$$

Pool fires are often tilted by wind, and even under strong winds, the base of a pool fire can be dragged downwind. The angle of the flame tilt, θ, can be calculated employing several methods of different difficulty. For example, American Gas Association (AGA, 1974) proposes a very simple correlation:

$$\begin{aligned} \cos\theta &= 1 \quad \text{for} \quad u^* \le 1 \\ \cos\theta &= \left(u^*\right)^{-0.5} \quad \text{for} \quad u^* \ge 1 \end{aligned} \tag{8}$$

More complex correlations which include the relationship between the tilt angle and the Reynolds and Froude numbers were introduced by Sliepcevich (1966).

Tab. 1. Pool fire flame length correlations.

Correlation Number	Correlation author	Equation	Wind speed dependence
1	Thomas (1963)	$\frac{L}{D}=42\left(\frac{m_B}{\rho_a\sqrt{gD}}\right)^{0,61}$	no
2	Thomas (1963)	$\frac{L}{D}=55\left(\frac{m_B}{\rho_a\sqrt{gD}}\right)^{0,67}u^{*\,0,21}$	yes
3	Moorhouse (1982)	$\frac{L}{D}=6,2\left(\frac{m_B}{\rho_a\sqrt{gD}}\right)^{0,254}u^{*\,-0,044}$	yes
4	Binding-Pritchard (1992)	$\frac{L}{D}=10,615\left(\frac{m_B}{\rho_a\sqrt{gD}}\right)^{0,305}u^{*\,-0,03}$	yes

Point source model and solid plume model geometry for pool fires

Point source model do not consider the shape of the pool fire, because the heat flux is assumed to originate from a point source located in the center of the pool fire. Therefore, the distance from the edge of the diked area, X, the diameter of pool, D, and the maximal flame height, L, are important parameters (Fig. 3). The distance of the point source to the receptor, x, can be calculated from the Pythagoras theorem as follows:

$$x=\sqrt{\left(\frac{L}{2}\right)^2+\left(\frac{D}{2}+X\right)^2} \tag{9}$$

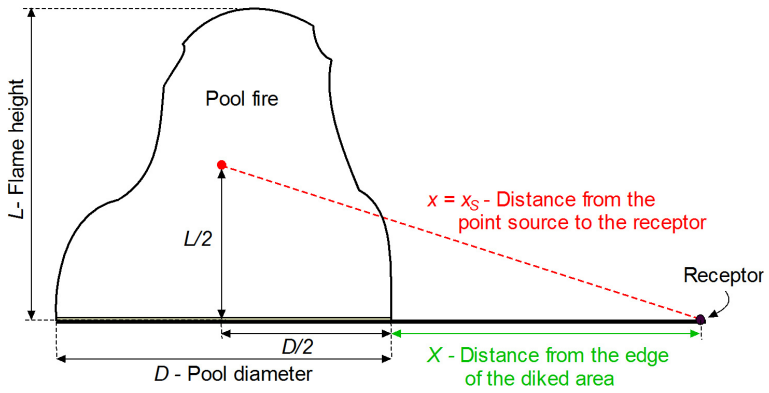

Fig. 3. Geometric layout of point source model in a pool fire.

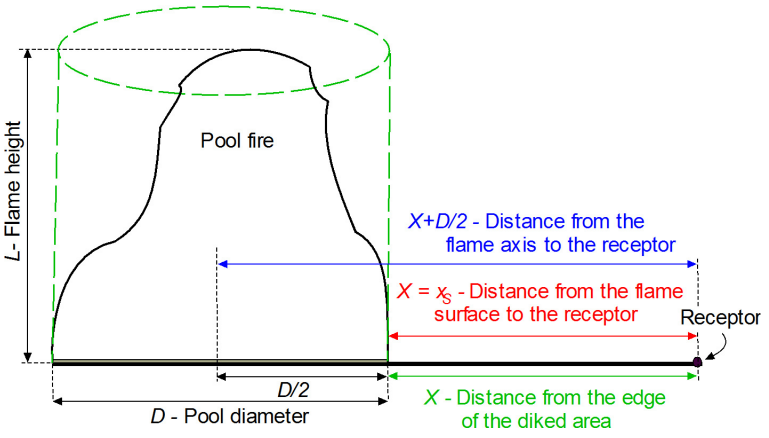

Fig. 4. Cylindrical geometric layout of pool fire for solid plume model.

This distance is subsequently used to calculate the atmospheric transmissivity and the geometric view factor.

The solid plume radiation model assumes that heat is radiated from the visible surface of a flame described as a solid object; however, invisible gases do not emit thermal radiation. Common geometries describing pool fire flames are: cylindrical flame, conical flame and cylindrical flame with elongated flame base diameter. If the solid plume radiation model is chosen, the distance from the flame surface to the receptor, X, and the distance from the flame axis to the receptor, $(X + D/2)$, are important parameters for the determination of atmospheric transmissivity and the geometric view factor (Fig. 4).

Energy radiated by the source and surface emitted power

Two different approaches for the estimation of the surface emitting power and radiating heat flux are available. The point source model is based on the assumption that energy radiated by the source, Q, is a fraction, F_S, (typical values from 0.15 to 0.35) of the total combustion energy produced by the combustion process, Q_C:

$$Q = Q_C F_s = \left(m_B A \Delta H_c\right) F_s \tag{10}$$

where A represents the pool area. The solid plume radiation model assumes that the visible volume of the flame emits thermal radiation. However, in case of pool fire, a large amount of soot is generated, which cover the visible flame and absorbs much of the radiation emitted. The fraction of the pool fire flame surface covered by soot, ς, is 0.8 and the emissive power of smoke, SEP_{soot}, is approximately 20 kW/m^2. Thus, the surface emissive power, SEP, is a combination of the maximum surface emissive power of "pure" flame, SEP_{max}, and the emissive power of smoke, SEP_{soot}:

$$SEP = (1-\varsigma) SEP_{\max} + \varsigma SEP_{soot} \tag{11}$$

The maximum surface emissive power of a flame without soot production is a function of the total combustion energy produced by the combustion process, Q_C, surface area of the flame, A_f, and a fraction of the combustion energy radiated from the flame:

$$SEP_{\max} = \frac{Q_c}{A_f} F_s = \frac{\left(m_B A \Delta H_c\right)}{A_f} F_s \tag{12}$$

Different approaches to the calculation of energy radiated by the source, Q, and the surface emitted power, SEP, result in differences not only in the values but also in the units of these parameters. The unit of the energy radiated by the source is J/s, but that of the surface emitted power is J/s/m^2.

Atmospheric transmissivity

Atmospheric transmissivity, τ_a, accounts for the emitted radiation being partly absorbed by air between the flame and the receptor. The main absorbing components in air are water vapor and carbon-dioxide. Pietersen and Huerta (1985) recommend a correlation formula that accounts for humidity:

$$\tau_a = 2.02\left(P_w x_S\right)^{-0,09} \tag{13}$$

where P_w represents partial pressure of water and x_S is the distance from the point source localized in the middle of the flame to the receptor if the point source model is considered, or it is the distance from the flame surface to the receptor if the solid plume radiation model is preferred.

Geometric view factor

The geometric view factor is the ratio between the received and the emitted radiation energy per unit area. The geometric view factor for the point source model, F_p, assumes that all radiation arises from a single point localized in the middle of the flame:

$$F_p = \frac{1}{4\pi x^2} \tag{14}$$

where x is the distance from the point source to the receptor. The geometric view factor for the point source model is given in m^{-2}.

For the solid plume radiation model, the geometric view factor, F_{21}, is determined by the flame dimensions, shape and the relative position and orientation of the receptor. Fig. 5 and 6 provide the view factors for untilted and tilted flames, respectively, for a ground level receptor from a radiation source represented by a circular cylinder. All equations for these figures were provided by Mudan and Croce (1988).

Heat flux at distance

Determination of the heat flux at a distance is dependent on the radiation model selected. If the point source model is selected, heat flux is determined from the energy radiated by the source, Q, atmospheric transmissivity, τ_a, (calculated using the distance from the point source) and the geometric view factor for the point source model, F_P:

$$E_r = Q \tau_a F_p \tag{15}$$

If the solid plume radiation model is selected, heat flux is determined from the surface emitted power, SEP, atmospheric transmissivity, τ_a, (calculated using the distance from the surface of the flame to receptor) and the geometric view factor for the solid plume radiation model, F_{21}:

$$E_r = SEP\, \tau_a F_{21} \tag{16}$$

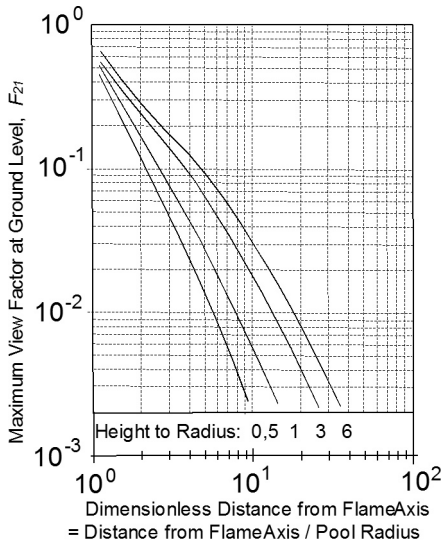

Fig. 5. Maximum view factors for a ground level receptor from a circular cylinder (Mudan and Croce, 1988).

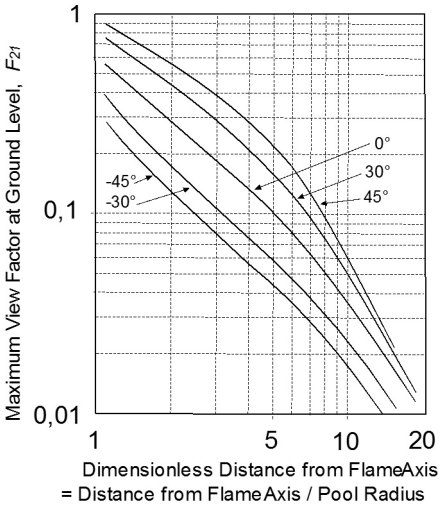

Fig. 6. Maximum view factors for a ground level receptor from a tilted circular cylinder (Mudan and Croce, 1988).

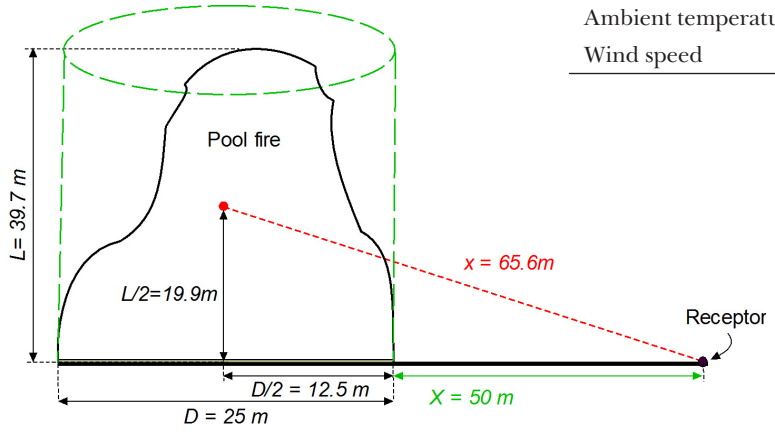

Fig. 7. Geometry of pool fire in still air conditions.

Estimation of thermal effect on receptor

Calculation of the thermal effect on receptor can be done in two ways. At first, if the receptor distance from the flames is known, calculation is straightforward and the result is a value of the heat flux at receptor in the required distance from the flame. Subsequently, for the selected duration of exposure, the probability of fatality can be determined.

On the other hand, it is more useful to know the distance from the flame at which the heat flux at receptor is secure or only a low probability of fatality exists. In this case, for the set heat flux, the corresponding value of distance between the receptor and the flame is calculated using an iterative method as many model parameters are depended on the distance between the flame and receptor.

Results and Discussion

Case study 1: Continuous release, still conditions

The first case study is oriented on calculation of radiation flux from a pool fire of high molecular hydrocarbon that escapes continuously from equipment at the volumetric rate of 0.1 $m^3 s^{-1}$ in still air conditions (windless day). A circular dike with a 25 m diameter stopped the enlargement of the pool although the equilibrium diameter of the burning pool would be larger. All necessary physico-chemical and meteorological parameters are summarized in Table 2.

Tab. 2. Input parameters for case study 1.

Flammable material parameters	Values	Units
Volumetric rate	0.1	$m^3 s^{-1}$
Boiling temperature	363	K
Density	730	kg m^{-3}
Heat of combustion	43 700	kJ kg^{-1}
Heat of vaporization	300	kJ kg^{-1}
Meteorological parameters	**Values**	**Units**
Relative humidity	50	%
Ambient temperature	298	K
Wind speed	0	m s^{-1}

To estimate the heat flux at a distance, point source model and solid plume radiation model were used. Burning rate, maximum pool diameter and flame length are parameters which are not affected by the choice of the radiation model. As the first parameter, the vertical burning rate was calculated using eq. (4). The knowledge of this parameter enables the determination of the maximum pool diameter caused by continuous leak (eq. (5)). Since the calculated maximal diameter was larger than the diameter of the diked area, the pool was constrained by the dike. Therefore, the area of the pool was calculated using the dike diameter. Since a windless day is expected, the Thomas correlation for still air conditions (Table 1) was used to estimate the pool fire flame length. Geometry of the pool fire in still air conditions with basic dimensions are depicted in Fig. 7. Other parameters needed to calculate the heat flux at a distance, are dependent on the type of the radiation model.

In case of a point source model, the distance of the point source to the receptor was calculated using the Pythagoras theorem (eq. (9)). This distance was used in eq. (13) for atmospheric transmissivity calculation and in eq. (14) for geometric view factor determination. Before the final calculation of the heat flux at the distance using eq. (15), the energy radiated by the point source has to be determined using eq. (10) and assuming the conservative value of 0.35 for the fraction of the energy converted to radiation. The unit of the energy radiated by the source is J/s and thus it can be combined only with the view factor for the point source model with the unit being m^{-2}.

The solid plume radiation model assumes that heat is radiated from the visible surface of a flame described as a cylinder with the dike diameter and flame length. Distance from the edge of the diked area to the receptor is equal to the distance from the flame surface to the receptor. This distance was used in eq. (13) for atmospheric transmissivity calculation and equally in the equations introduced by Mudan and Croce (1988) for the view factor for untilted flames. Since the fuel is a high molecular weight material, a sooty flame is expected. Hence, using eq. (11) to calculate the surface emissive power, the fraction of the flame surface covered by soot of 0.8 was assumed. Final heat flux for the solid plume radiation model was calculated using eq. (16).

Table 3 provides the output parameters at the distance of 50 m from the edge of the diked area. Fig. 8 presents heat flux predicted by the point source model and the solid plume model as a function of the distance from the edge of the dike area to the receptor in the range of 0 to 200 m. From Fig. 8 it follows that, compared with the solid plume model, the point source model predicted higher heat flux at receptor mainly for shorter distances from the edge of the dike area. This overestimation of heat flux leads to considerably conservative prediction of the thermal effect on receptor. In this case study, a good agreement of the heat flux predicted by the point source model and that predicted by the solid plume model was observed in the distance of about 75—100 m, which corresponds to the distance of about 3—4 pool diameters from the edge of the diked area.

Case study 2: Instantaneous release, wind conditions

The second case study was focused on the calculation of radiation flux from a burning pool caused by an instantaneous release of 28.3 m^3 of petrol with the thickness of about 0.02 m. In this case study,

Tab. 3. Numerical output parameters of case study 1 at the distance of to 50 m from the edge of the diked area.

Vertical rate of liquid level, $\dot{y}_{max}$		1.2×10^{-4} m s^{-1}	
Burning rate, m_B		0.0876 kg m^{-2} s^{-1}	
Maximum diameter, D_{max}		32.6 m	
Diameter of dike area, D		25 m	
Area of pool, A		490.6 m^2	
Flame length, L		39.7 m	
Distance from edge of diked area to receptor, X		50 m	
Point Source Model		**Solid Plume Model**	
Distance from the point source to receptor, x	65.6 m	Distance from the flame surface to receptor, X	50 m
Energy radiated by the source, Q	657.3 MJ s^{-1}	Surface Emitted Power, SEP	52.4 kJ m^{-2} s^{-1}
Atmospheric transmissivity, τ_a	0.7144	Atmospheric transmissivity, τ_a	0.7321
Geometric view factor, F_p	1.85×10^{-5} m^{-2}	Geometric view factor, F_{21}	0.0758
Heat flux at Distance, E_r	8.69 kJ m^{-2} s^{-1}	Heat flux at Distance, E_r	2.91 kJ m^{-2} s^{-1}

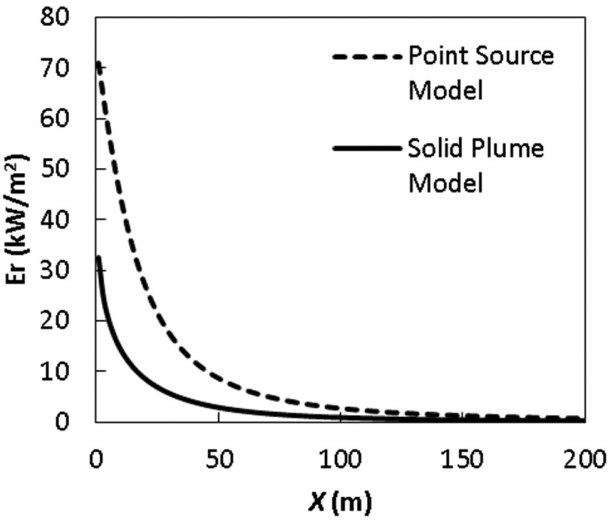

Fig. 8. Heat flux as a function of the distance from the flame surface to the receptor. Comparison of point source and solid plume model prediction.

different wind speeds were taken into account. All necessary physico-chemical and meteorological parameters are summarized in Table 4.

Tab. 4. Parameters in case study 2.

Flammable material parameters	Values	Units
Volume	28.3	m^3
Average pool thickness	0.02	M
Boiling temperature	423	K
Density	720	kg m^{-3}
Heat of combustion	45 000	kJ kg^{-1}
Heat of vaporization	366	kJ kg^{-1}
Heat capacity	2.2	kJ kg^{-1} K^{-1}
Meteorological parameters	**Values**	**Units**
Relative humidity	70	%
Ambient temperature	288	K
Wind speed	0, 1, 5, 8	m s^{-1}

According to the logic diagram for pool fire radiation effects calculation (Fig. 2), the burning rate was determined first. Because of sufficient experimental data for petrol pool fire, the Zabetakis-Burgess method for burning rate determination (eq. (2)) could be used. At the petrol parameters $m_{B\infty}$ = 0.055 kg s^{-1} m^{-2} and $k \times \beta$ = 2.1 m^{-1}, the burning rate of 0.055 kg s^{-1} m^{-2} was obtained. Burning rate calculated using the Burgess-Strasser-Grumer method (eq. (3)) was equal to 0.0619 kg s^{-1} m^{-2}. The difference between the obtained burning rates is in this case slightly above 10 %. For the following calculation, the value of 0.055 kg s^{-1} m^{-2} was used because of the very good agreement with published experimental data for petrol. Considering an instantaneous leak of flammable material, the pool diameter was calculated using eq. (6). Pool fire flame length was calculated using all four correlations listed in Table 1. The obtained flame lengths are summarized in Table 5. Fig. 10 shows the flame length as a function of the pool fire diameter using all mentioned correlations. For correlations allowing including the wind speed dependence, the wind speed equal to 5 m s^{-1} was used in the calculations. As it can be seen in Table 5 or Fig. 10, differences in the flame length predicted by different correlations are significant. The Thomas correlation for still air conditions is, because of its simplicity, often used if a point source model is chosen for heat flux prediction. Correlations including the wind speed dependence (Thomas, 1963; Moorhouse, 1982; Binding-Pritchard, 1992) are used mainly for flame geometry determination in the solid plume radiation model. Because the Thomas correlation with wind speed dependence usually underestimates the length of the flame (Assael, 2010) and the flame lengths predicted by the Binding-Pritchard correlation are too high for a large pool diameter, the Moorhouse method was chosen for further calculation.

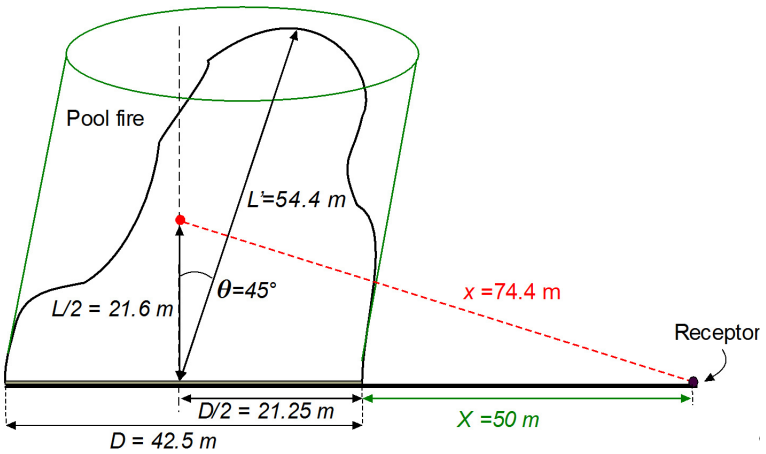

Fig. 9. Geometry of pool fire in strong wind conditions.

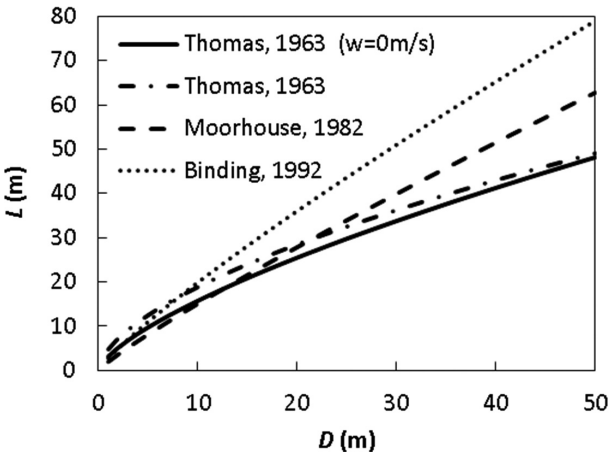

Fig. 10. Flame length as a function of pool fire diameter calculated by different semi-empirical correlations.

Another important parameter in flame shape determination is the flame tilt. Assuming the wind speed of 5 m/s, the angle of flame tilt was determined using a very simple correlation proposed by AGA and a correlation including the relationship between the tilt angle and the Reynolds and Froude numbers provided by Sliepcevich (1966). As it is summarized in Table 5, a good agreement of the results for the flame tilt angle of 43° or 45° was achieved by various correlations. Other calculation procedures depend on the type of the radiation model selected. In case of a point source model, the effect of the wind on the flame geometry was omitted (see Fig. 9). The distance of the point source to the receptor was calculated using the flame length calculated by the Thomas correlation for still air conditions; the flame tilt in the wind direction was also omitted. Thus, the obtained distance was applied to eq. (13) to determine the atmospheric transmissivity and in eq. (14) to determine the geometric view factor for the point source model. Energy radiated by the point source was determined using eq. (10) assuming that the fraction of the energy converted to radiation is equal to 0.2. Final heat flux at the distance was calculated using eq. (15). The solid plume radiation model assumes that heat is radiated from the surface of a cylinder which tilts in the wind direction (see Fig. 9). The distance from the flame surface to the receptor was used in eq. (13) to calculate atmospheric transmissivity and also in the equations provided by Mudan and Croce (1988) for the view factor for tilted flames. Providing that 80 percent of the flame surface are covered by soot, the surface emissive power was calculated by eq. (11). Final heat flux for the solid plume radiation model was calculated using eq. (16).

Table 5 provides the output parameters at the distance from the edge of the diked area to the receptor of 50 m and the wind speed of 5 m s^{-1}. Fig. 11 compares the heat flux predicted by the point source model and heat fluxes predicted by the solid plume model for different wind speeds as a function of the distance from the edge of the dike area to the receptor. From Fig. 11 it follows that thermal radiation to

Tab. 5. Numerical output parameters of case study 2 at the distance of 50 m from the edge of the diked area.

Wind speed, u_w		5 m s^{-1}	
Burning rate, m_B (Zabetakis & Burgess, 1961)		**0.055 kg m^{-2} s^{-1}**	
Burning rate, m_B (Burgess et al., 1961)		0.0619 kg m^{-2} s^{-1}	
Diameter of pool, D		42.5 m	
Area of pool, A		1415 m^2	
Flame length, L (Thomas, 1963, still air)		43.2 m	
Flame length, L (Thomas, 1963)		44.8 m	
Flame length, L (Moorhouse, 1982)		**54.4 m**	
Flame length, L (Binding-Pritchard, 1992)		68.84 m	
Angle of flame tilt, θ (AGA, 1974)		43°	
Angle of flame tilt, θ (Sliepcevich, 1966)		**45°**	
Distance from edge of diked area to receptor, X		50 m	
Point Source Model		**Solid Plume Model**	
Distance from the point source to receptor, x	74.4 m	Distance from the flame surface to receptor, X	50 m
Energy radiated by the source, Q	700.4 MJ s^{-1}	Surface Emitted Power, SEP	32.2 kJ m^{-2} s^{-1}
Atmospheric transmissivity, τ_a	0.7247	Atmospheric transmissivity, τ_a	0.7511
Geometric view factor, F_p	1.44×10^{-5} m^{-2}	Geometric view factor, F_{21}	0.27
Heat flux at Distance, E_r	7.3 kJ m^{-2} s^{-1}	Heat flux at Distance, E_r	6.5 kJ m^{-2} s^{-1}

receptor at a defined downwind distance increases with the wind speed.

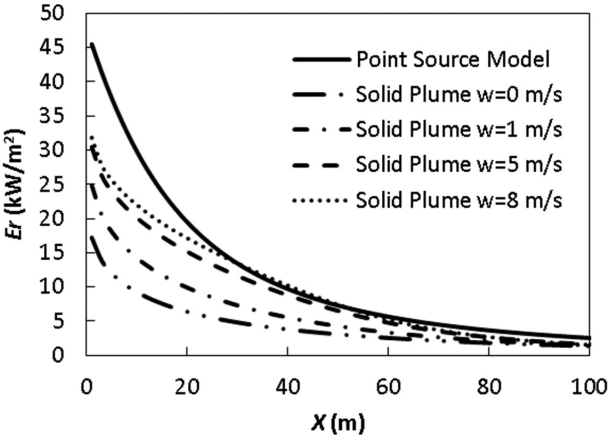

Fig. 11. Radiant flux as a function of the distance between the flame surface and the receptor for different wind speeds calculated using the solid plume model and the point source model.

For higher speed of wind, the heat flux predicted by the solid plume model is in a good agreement with that predicted by the point source model which does not depend on the wind speed in the accident area. Assuming wind speed of 5 m/s, the point source model and the solid plume model are in good agreement considering the distance of about 1 radius from the edge of the diked area. One of the basic problems with the inclusion of wind in the calculation of heat flux on receptor is often a change of its speed and direction. Potential underestimation of the heat flux can endanger the lives of persons intervening in the area of accident.

Conclusions

By their nature, semi-empirical models depend strongly on experimental data. Correlations are able to describe the general features of a fire. Semi-empirical models are ideally suitable for routine hazard assessment because they are mathematically simple, and hence easily understood. However, if more models describing the same phenomenon are available, significant differences in the heat flux prediction can be expected. The point-source models do not consider the shape of the flame but they assume that the heat flux originates from a point source. These models usually overestimate the heat flux in a short distance from the pool fire flames which leads to considerably conservative prediction of the thermal effect on receptor. The solid flame models assume that the flame is of a solid shape radiating heat from its surface and take into account the coverage of visible flame with soot and wind speed in the affected area. However, for higher wind speed, heat flux predicted by the point source model is in good agreement with the heat flux predicted by the solid plume model and the overestimation is not significant. Because semi-empirical models depend strongly on experimental data of different authors and more submodels describing the same phenomenon (flame length, flame tilt...) are available in literature, significant differences in the parameter prediction can be expected. Therefore, a critical evaluation and comparison of the obtained results is always necessary.

Acknowledgment
This work was supported by the Slovak Scientific Agency, Grant No. VEGA 1/0749/15.

References

AGA (1974) IS 3-1: LNG Safety Research Program, Columbus, OH: American Gas Association.

Assael MJ, Kakosimos KE (2010) Fires, Explosions, and Toxic Gas Dispersions: Effects Calculation and Risk Analysis, CRC Press 2010, eBook ISBN: 978-1-4398-2676-8.

Binding TM, Pritchard MJ (1992) Fire2: A new Approach for predicting Thermal Radiation Levels from Hydrocarbon Pool Fires, I. Chem E Symposium Series No. 130, Volume 3.

Burgess DS, Strasser A, Grumer L (1961) Diffusive Burning of Liquid Fuels in Open Trays, Fire Res. Abstr. Rev. 3: 177.

CRP 14E (Part 2) (1997) Methods for the Calculation of Physical Effects – due to releases of hazardous materials (liquids and gases) – "Yellow Book", Committee for the Prevention of Disasters. ISBN 90-12-08497-0.

Eisenberg NA, Lynch CJ, Breeding RJ (1975) Vulnerability Model: A Simulation for Assessing Damage Resulting from Marine Spills, US Coast Guard, AD/A015 245, NTIS Report No. CG-D-137-75.

GCPQRA (2000) Guidelines for Chemical Process Quantitative Risk Analysis, 2nd Edition, New York: American Institute of Chemical Engineers.

Lees FP (1994) The Assessment of Major Hazards: A Model for Fatal Injury From Burns, Trans. IChemE, Vol. 72, Part B.

Moorhouse J (1982) Scaling Criteria for Pool Fires Derived From Large-Scale Experiments, I. Chem. Sym. Ser., Vol. 71, pp. 165–79.

Mudan KS (1985) Thermal Radiation from Hydrocarbon Pool and Vapor Fires, Arthur D. Little Inc. Report 50688.

Mudan KS, Croce PA (1988) Fire Hazard Calculations for Large Open Hydrocarbon Fires, SFPE Handbook of Fire Protection Engineering. Boston, MA: Society of Fire Protection Engineers.

Pietersen CM, Huerta SC (1985) TNO 84-0222: Analysis of the LPG Incident in San Juan Ixhuatepec, Mexico City, 19 Nov 1984, Apeldoorn, The Netherlands: Netherlands Organization for Applied Scientific Research.

Sliepcevich CM, Welker JR (1966) Bending of wind-blow flames from liquid pools, Fire Technology 2, pp. 127—135.
Thomas PH (1963) The Size of Flames From Natural Fires, 9th Interactional Symposium on Combustion, New York: Academic Press.
Zabetakis MG, Burgess DS (1961) Research on the Hazards Associated with the Production and Handling of Liquid Hydrogen, R.I. 5707, Bureau of Mines, Pittsburgh.

List of symbols

A	pool area	m^2
A_f	flame surface area	m^2
C_p	heat capacity	J kg^{-1} K^{-1}
D	pool diameter	m
E_r	heat flux	kJ m^{-2} s^{-1}
F_S	fraction of the energy converted to radiation	
F_p	view factor for the point source model	m^{-2}
F_{21}	view factor for the solid plume model	
g	gas constant	J mol^{-1} K^{-1}
ΔH_c	heat of combustion	J kg^{-1}
ΔH_v	heat of vaporization	J kg^{-1}
k	absorption extinction coefficient of the flame	m^{-1}
L	flame length	m
m_B	burning rate	kg s^{-1} m^{-2}
$m_{B\infty}$	burning rate of an infinite diameter pool	kg s^{-1} m^{-2}
P_w	partial pressure of water	Pa
Q	energy radiated by the source	J s^{-1}
Q_C	total combustion energy	J s^{-1}
SEP	surface emitted power	J s^{-1} m^{-2}
SEP_{max}	maximum surface emissive power	J s^{-1} m^{-2}
SEP_{soot}	emissive power of smoke	J s^{-1} m^{-2}
T_{BP}	boiling point temperature	K
T_a	ambient temperature	K
T_f	flame temperature	K
u^*	nondimensional wind speed	
u_w	wind speed	m s^{-1}
V_L	volume of flammable material	m^3
$\dot{V}_L$	volumetric leak rate	m^3 s^{-1}
x	distance of the point source to receptor	m
x_S	distance for atmospheric transmissivity calculation (eq. 13)	m
X	distance from the flame surface to receptor	m
$\dot{y}_{max}$	vertical rate of liquid level decreases	m s^{-1}
Greek symbols		
β	mean beam length corrector in eq.	
δ	poll thickness	m
ε	grey-body emissivity	
θ	angle of flame tilt	°
ρ_a	air density	kg m^{-3}
ρ_V	density of fuel vapor	kg m^{-3}
ρ_{liq}	fuel density	kg m^{-3}
σ	Stefan-Boltzmann constant, 5.6703×10^{-8} J s^{-1} m^{-2} K^{-4}	
ς	fraction of the surface of the pool fire flame covered by soot	
τ_a	atmospheric transmissivity	